

Development of a Hybrid Index for Drought Prediction: Case Study

Mohammad Karamouz¹; Kabir Rasouli²; and Sara Nazif³

Abstract: Drought is a natural phenomenon that occurs in many places on the planet and may cause considerable damage. Selection of an integrated index for quantifying drought severity is a challenge for decision makers in developing water resources and operation management policies. In this study, the standardized precipitation index, water surface supply index, and Palmer drought severity index have been combined to develop an integrated index, called the hybrid drought index (HDI), using associated damage of drought events. Application of the HDI in drought severity prediction has been examined using two different types of artificial neural networks, namely, a probabilistic neural network and a multilayer perceptron network. These models have been selected due to their special characteristics that are suitable for prediction schemes. The proposed algorithm for developing HDI and drought prediction has been applied to the “Gavkhoni/Zayandeh-rud” basin in the central part of Iran. The results show the merits of each model in prediction of drought severity and model adaptation. The results also show the significant value of the proposed algorithm in formulation of a combined index for drought prediction.

DOI: 10.1061/(ASCE)HE.1943-5584.0000022

CE Database subject headings: Droughts; Predictions; Neural networks; Hybrid methods.

Introduction

Drought occurs in every climate with varying frequency and characteristics. Drought damages could be high in regions with high water supply dependencies and cause serious regional impact. Therefore, prediction of drought severity in order to reduce its adverse effects is essential. In fact, there are many supply and demand issues that should be considered in evaluating the severity of droughts, depending on the perception of end users and others involved—such as hydrologists, meteorologists, water resources engineers, agricultural researchers, economists, and a wide range of stakeholders. Dracup et al. (1980) stated that it is not possible to define and analyze droughts without paying attention to the nature of the water shortage. They used truncation levels such as long-lead average in order to diagnose the dry and wet periods in historical time series of river flow. It is important to note that the indications of drought should be strong enough to prevent misleading signals.

Initial studies of drought aspects have been done by Palmer (1965) who used the meteorological parameters and soil moisture properties in order to define the indices for determining the drought severity and duration. He also developed an index of moisture anomaly Z index and Palmer drought severity index

(PDSI). This pioneering study followed by many other state of the art studies is frequently cited in the literature. Pinkayan (1966), Dracup et al. (1980), Sen (1980), Santos et al. (1983), Rouhani and Cargile (1989), and Shin and Salas (2000) should be seen for more details. A number of climatic and hydrological variables, such as precipitation, streamflow, soil moisture, groundwater levels, and moisture content in the air, have been widely used in the literature for characterizing different aspects of drought. Precipitation has been commonly used for meteorological drought analysis (Tase 1976; Eltahir 1992; Karamouz et al. 2007), while streamflow data have been widely applied for hydrologic drought analysis (Zelenhasic and Salvai 1987; Wang and Salas 1989; Chang 1990; Frick et al. 1990; Clausen and Pearson 1995; Karamouz et al. 2004b). The purpose of this paper is to propose a hybrid index of drought severity that can be used as a tool for drought monitoring and prediction in an integrated fashion.

The hybrid drought index (HDI) has been developed by combining the three important indices of meteorological, hydrological, and agricultural droughts, namely, standardized precipitation index (SPI) (McKee et al. 1993), surface water supply index (SWSI) (Shafer and Dezman 1982), and PDSI by utilizing the drought damage data. The data obtained from drought damage is a good indicator of combined drought severity and include all aspects of their gradual and longer term impacts. Therefore, it can be used to identify the combined effects of drought and to analyze its variability in order to develop preventive schemes and reduce drought impacts on different water user sectors.

For predicting the characteristics and the impacts of droughts, there are different simple simulation models, such as regression, autoregressive (AR) based models as well as artificial neural networks (ANNs). ANNs can estimate the linear and nonlinear behavior of complicated systems which cannot be explained using relatively straightforward mathematic relations. ANNs identify these relations during the learning stage. Different types of neural networks have been developed and applied for prediction of the complicated phenomena in different fields of science. Shin and

¹Professor, School of Civil Engineering, Univ. of Tehran, Enghelab Ave., Tehran, Iran (corresponding author). E-mail: karamouz@ut.ac.ir

²MSc, Engineering Dept., Islamic Azad Univ. Science & Research Branch of Tehran, Tehran, Iran. E-mail: kabir.rasouli@gmail.com

³Ph.D. Candidate, School of Civil Engineering, University of Tehran, Tehran, Iran. E-mail: snazif@ut.ac.ir

Note. This manuscript was submitted on August 29, 2007; approved on September 5, 2008; published online on February 18, 2009. Discussion period open until November 1, 2009; separate discussions must be submitted for individual papers. **This paper is part of the *Journal of Hydrologic Engineering*, Vol. 14, No. 6, June 1, 2009. ©ASCE, ISSN 1084-0699/2009/6-617-627/\$25.00.**

Salas (2000) analyzed regional droughts using neural networks. In that study, an approach for analyzing and quantification of spatial and temporal patterns of meteorological droughts has been developed using annual precipitation.

Multilayer perceptron networks (MLPs) are among the most popular ANNs. The MLP models have been used for drought and flood predictions in the literature. Karamouz et al. (2004a) have used different neural networks in flood prediction. They indicated that the MLP provides better results for extreme events than the recurrent and time delay networks because they are less data intensive.

Recently, the applications of the ANN models with probabilistic base have received more attention. Probabilistic neural networks (PNNs) are the supervised type of neural networks which are based on Bayesian rule and are widely used in the area of pattern recognition, nonlinear mapping, and estimation of the probability of class membership and likelihood ratios (Specht and Romsdahl 1994; Cohen and Intrator 2002; and Miravet and Rodriguez 2003). These models due to their probabilistic basis can be efficient in the classification of common states of variables into specified groups (i.e., classification of dry and wet months or different drought severity ranges). The PNN models can generalize the results and can estimate the anomalies. However, their applications are fairly new in water resources management studies.

The PNN may require more neurons than standard feed-forward back propagation networks, but often it can be developed in a fraction of the time that it takes to train a standard feed-forward network (see Chen et al. 1991). In this study, due to the specific characteristics of MLP and PNN models, they have been used for predicting the proposed hybrid index.

In the next sections, a methodology for development of a HDI is introduced. Then, the governing factors that play an important role in assessment of drought damage are explained. A discussion on the two ANN models is followed and the study area is described. Finally the results are discussed and a "Summary and Conclusions" section is presented.

Methodology

In this study, an integrated drought index has been developed for evaluating drought impacts. In many drought studies, the focus has been on agricultural droughts due to vulnerability of crops in severe droughts. PDSI, as the most important index of drought evaluation, has been considered in many studies but there are some shortcomings in the way it is determined. This index is sensitive to the available water capacity (AWC) of soil but for simplification of index computations, soil properties are considered to be similar in different layers of soil. Furthermore, the lag time between precipitation and the resulting runoff is not considered which leads to an inaccurate estimation of index (Alley 1984). Potential evapotranspiration is usually estimated using a water balance model such as the Thornthwaite method.

The other index used in this study is the SWSI which is an important index for hydrological droughts. The SWSI is very sensitive to general characteristics of the basin. For example, dam construction in a basin can change the sequence of water availability. In this situation, SWSI indices from before and after dam construction are not comparable. This could yield to misclassification of historical drought severity.

The third drought index which has been studied in this paper is the SPI developed by McKee et al. (1993). It is based on the

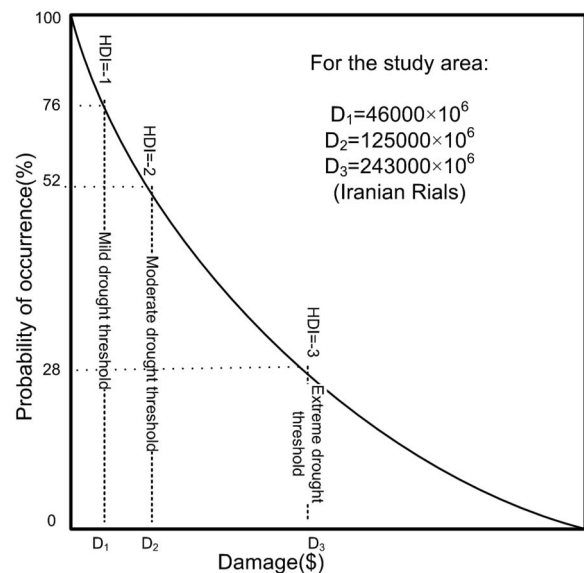


Fig. 1. Diagram of cumulative probability of historical damages and thresholds of different drought severity

probability of precipitation for any time scale which provides early drought warning. The SPI is easier to deal with than the other two indices. In calculating the SPI, a gamma distribution is fitted to the observed precipitation values during 1, 3, 6, 9, 12, 24, or 48 month periods (1 month is used in the present study). The gamma distribution is then transformed to a Gaussian distribution (standard normal distribution with mean zero and variance of one), which gives the value of the SPI for the appropriate time scale.

Positive SPI values indicate greater than median precipitation, while negative values indicate less than median precipitation. The fact that drought indices have some shortcomings does not mean that they are not reliable tools for drought assessing but shows that their shortcomings can be improved by utilizing the others in a hybridized form such as HDI. Therefore, hybridizing the indices could cover the combined impacts of different factors affecting drought severity. Here, PDSI, SWSI, and SPI have been combined through the analysis of drought damage as a new approach for quantifying drought impacts. Drought damage is selected because it is the result of all aspects of meteorological, hydrological, and agricultural droughts. Therefore, one may consider a relation to estimate the drought damage as follows:

$$\text{Damage}_t = f(\text{SPI}_{t-1}, \text{SWSI}_{t-1}, \text{PDSI}_{t-1}) \quad (1)$$

Because of the difficulties in determining the function f in Eq. (1), ANN models are applied. Estimating the damage based on SPI, SWSI, and PDSI, the HDI has been developed in this study. The framework of the adjusted SWSI-index developed by Garen (1993) has been adapted in the definition of the HDI according to Eq. (2).

$$\text{HDI}_t = f(\text{Damage}_t) = \frac{P_t(\text{Damage}) - 100}{24} \quad (2)$$

where P_t = cumulative probability of damage in month t . Fig. 1 shows the schematic cumulative probability of damage and its relation to the HDI. The characteristics of the damages for the three types of droughts are complex with a significant degree of nonlinearity and uncertainties. Therefore, for analyzing the nonlinear relations between them, the ANN models are applied in this

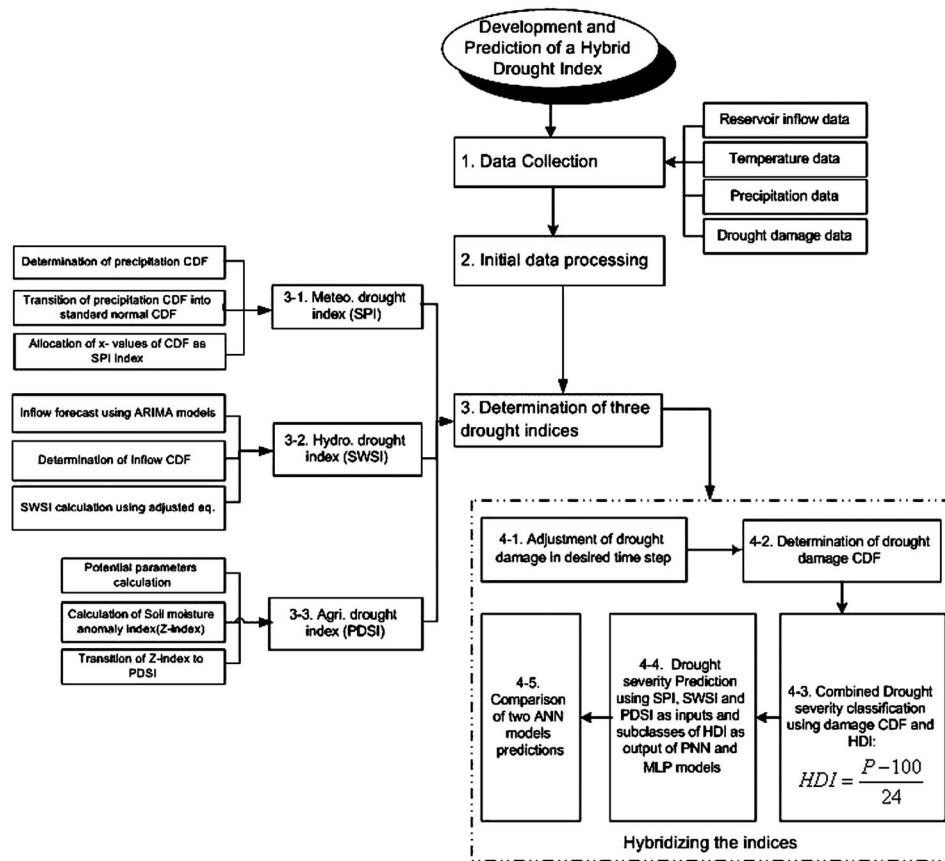


Fig. 2. Algorithm for calculation of hybrid drought index (HDI)

study. Simple methods such as regression or autoregression models only give rough estimates for drought damage and the resulting HDI. The following regression model has been developed for the HDI in this study:

$$HDI_t = -1.94 - 0.0554PDSI_{t-1} + 0.499SPI_{t-1} + 0.106SWSI_{t-1} \quad (3)$$

which yields to $R^2=21.6\%$ which is quite low and shows the unreliability of the equation. The efficiency of implementing a robust training system such as artificial neural networks, especially those with a probabilistic background, has been tested in the estimation of drought indices in relation to the HDI.

The following steps are carried out for HDI determination and utilization for the drought severity prediction using the artificial neural networks:

1. Calculation of time series of SPI, SWSI, and PDSI as indices for meteorological, hydrological, and agricultural aspects of droughts;
2. Analysis and adjustment of historical drought damage data and estimating the monthly damage;
3. Finding the most appropriate cumulative probability distribution that fits the historical monthly damages (Fig. 1);
4. Determination of the HDI values from the cumulative probability of damages [Eq. (2)];
5. Classification of the HDI values into subcategories that Class 1 and the last class denote to the normal and extremely severe drought conditions, respectively; and
6. Estimation of HDI subcategories and consequently the range of drought damage through calculated indices of different drought types by training a system.

It should be mentioned that two types of ANN models have been used, namely MLP networks and PNN for training. SPI, SWSI, and PDSI for the current time scale are the network inputs and the HDI subcategories specified in Step 5 for the next time scale are their outputs. The 1 month time delay between drought indices and HDI is considered because of the lag time between the occurrence of drought and its consequences.

Once ANNs are trained, simply having the field observations of rainfall, temperature, reservoir inflow, and soil moisture, the values of HDI can be estimated. Obviously, the range of probable damage can be obtained using upper and lower bounds of the HDI subcategories and Eq. (2). The flowchart of the proposed approach for determining the HDI is shown in Fig. 2.

In comparison to the SWSI, HDI is utilized only for evaluation of dry spans (unlike SWSI, HDI has only negative values, so it can be used only for drought classification). The HDI values vary within $(-4, 0)$ which makes it comparable with other indices of drought such as SWSI.

According to the HDI, drought starts when the HDI goes below -2 and continues unless it reaches above -1 . The reason for selecting -2 as a threshold of drought beginning is that when the HDI is above -2 , as it is shown in Fig. 1 for the study area, there is no significant change in the amount of damage, especially for HDI values greater than -1 . It can also be mentioned that at the beginning of drought spells, observed impacts are not very much due to gradual occurrence of droughts.

Classification of Hybrid Drought Index

There are four main categories of drought severity according to the HDI: negligible, mild, moderate, and extreme severity. This

Table 1. Classification of Drought Severity Based on Hybrid Drought Index (HDI)

Drought	Number subclass	HDI interval	Average of HDI
Negligible severity	1	$-0.25 < \text{HDI} < 0$	-0.125
	2	$-0.5 < \text{HDI} \leq 0.25$	-0.375
	3	$-0.75 < \text{HDI} \leq 0.5$	-0.625
	4	$-1 < \text{HDI} \leq 0.75$	-0.875
Mild	5	$-1.25 < \text{HDI} \leq 1$	-1.125
	6	$-1.5 < \text{HDI} \leq 1.25$	-1.375
	7	$-1.75 < \text{HDI} \leq 1.5$	-1.625
	8	$-2 < \text{HDI} \leq 1.75$	-1.875
Moderate	9	$-2.25 < \text{HDI} \leq 2$	-2.125
	10	$-2.5 < \text{HDI} \leq 2.25$	-2.375
	11	$-2.75 < \text{HDI} \leq 2.5$	-2.625
	12	$-3 < \text{HDI} \leq 2.75$	-2.875
Extreme severe	13	$-3.25 < \text{HDI} \leq 3$	-3.125
	14	$-3.5 < \text{HDI} \leq 3.25$	-3.375
	15	$-3.75 < \text{HDI} \leq 3.5$	-3.625
	16	$-4 < \text{HDI} \leq 3.75$	-3.875
	17	$\text{HDI} \leq 4$	-4.125

classification of drought which is shown in Table 1, is based on the cumulative probability of drought damage. For damages with the cumulative probability and the HDI value of less than 25% and -1, respectively, drought severity is considered to be negligible. This is because of the fact that damage exists but it is not significant enough to be attributed only to drought occurrence. When the value of HDI reaches -2, the damage caused by drought is moderate and it can be assumed that drought span starts. Finally when the value of HDI reaches -3, different water users, especially agriculture and animal husbandry sectors, suffer from water shortages and it is considered the critical stage of drought.

In regions where drought damages are generally high, small climate changes may cause extensive variations in damages. Therefore in these regions, in order to evaluate the variations of drought impact, the classification of drought severity in smaller intervals can be helpful. For more accurate evaluation of drought, each of the four major categories of drought severity obtained through the HDI classification, has been divided into four subcategories except the fourth category which has five subcategories considering the fact that values less than -4 might be predicted by the neural networks (see Table 1). As a result, 17 subcategories have been defined according to the cumulative probability of drought damages. The output of ANN models, which are used for drought severity prediction as discussed in the next section, is the expected value of HDI subcategory.

Evaluation of Water Availability and Drought Damages

Damages caused by drought depend on water availability and demands and is significant in the areas that have demands greater than water supply. In order to assess the effect of water shortage on different water users, damage (loss of property and life) data which is usually reported in the annual time scale has been converted to monthly time series considering the role of water demands and agricultural parameters (i.e., crop type and coverage area as well as its sensitivity to soil water shortages) in

damage value in a given month during the droughts. Moreover, reservoir storage and its releases have direct effects on the extent of damage.

In this paper, the effective variables in the damage assessment have been considered in two categories. The first involves the agricultural related variables [Eq. (4)] and the others address the water availability [Eq. (6)]. The variables such as crop coverage and type of crops, and the crop sensitivity to the water shortages ($K_y^{i,j}$) in different stages of growth have been considered in the assessment of drought damages. These variations are coupled into a coefficient of agricultural damage (AD) according to the following equation:

$$\text{AD}_i = \frac{B_i}{\sum_{i=1}^{12} B_i} \times 100 \quad (4)$$

and

$$B_i = \frac{\sum_{j=1}^m K_y^{i,j} A_{i,j}}{\sum_{j=1}^m A_{i,j}} \quad (5)$$

where AD_i =ratio of agricultural damage for month i to the annual damage (%); $A_{i,j}$ =crop j coverage area in month i ; $K_y^{i,j}$ =crop j sensitivity to soil water shortages; B_i =coefficient of the crop yield which is the weighted mean of $K_y^{i,j}$ based on the crop coverage area; and m =number of crops in the region. Calculating AD_i for every month of a year, one can find the critical months in the study area during which agricultural crops are vulnerable to drought. This is used to obtain the associated damage of each month out of annual damage.

According to the definition of $K_y^{i,j}$ when its value is 1 for a specified crop during one of its growth stages, for any one unit deficit in its water demand, the final crop yield will be decreased by one unit. The lower crop yield, $K_y^{i,j}$ varies during different stages of its growth.

The other category called water availability (WA) of the reservoir has been considered in the evaluation of drought damage which controls the allocation of water to different sectors. For this purpose, the whole water demands of agricultural, industrial, domestic, and environmental sectors (instream flow) for every month of a normal year have been defined as WD and it is combined with a factor, Q'_i , that justifies the role of reservoir in supplying the demands as follows:

$$\text{WA}_i = \frac{\text{WD}_i \cdot Q'_i}{\sum_{i=1}^{12} \text{WD}_i \cdot Q'_i} \times 100 \quad (6)$$

$$Q'_i = 1 - \frac{Q_i}{Q_{\max}} \quad (7)$$

where Q_i and Q_{\max} =monthly and maximum reservoir outflows, respectively; and Q'_i is used as the water deficit penalty coefficient in computing the monthly damage, and varies between 0 and 1 for the highest and lowest reservoir outflows.

WA_i shows that when the reservoir inflow in month i increases, the vulnerability of different sectors to water shortages and then the probable damage of drought will decrease. Also, it shows that when water demand (WD) during a month increases, water shortages cause more damage. Combining Eqs. (4) and (6), one may obtain an expression for determining the percentage of monthly damages (MD) as

$$MD_i = \frac{WA_i \cdot AD_i}{\sum_{i=1}^{12} WA_i \cdot AD_i} \times 100 \quad (8)$$

Using Eq. (8), drought damage of each month is determined. Drought damage is a function of the physical conditions, and also of social settings. It seems that social settings change over time, particularly as experience accumulates. For example social response in an early drought is not likely to be the same compared with a later drought, and therefore different drought damage for two sequential droughts having similar physical characteristics is possible and the reported damages are different than the actual values. For representing the variability in social settings and estimating the real damages an adjusting coefficient, $\alpha_m(i)$ is introduced. This causes the damage to be reduced for later droughts in comparison to earlier droughts as the experience of dealing with droughts accumulates. Therefore, reported values of damage are adjusted by coefficient, $\alpha_m(i)$. Consider that there have been n dry months in a given drought in the basin preceded by another drought, a social setting factor $\alpha_m(i)$ for dry month i in the m th drought could be formulated as a parabola function as follows:

$$\alpha_m(i) = ai^2 + bi + c + d\alpha_{m-1}(n_{m-1})c = 1, \quad i = 1, 2, 3, \dots, n_m \quad (9)$$

where $\alpha_{m-1}(n_{m-1})$ =social setting factor for the last month of the previous drought. This term shows that as the previous experience of drought accumulates the social preparedness to cope with the incoming droughts improves and the associated damage decreases. In this study, to determine a and b , it is assumed that $\alpha_0(n_0)$ is zero and the damage is decreased by 10% at the end of the drought period. d could be selected based on the regional social response to damage reduction. It is assumed to be 0.2 in this study. The parabola function is selected to show that the effect of social experience on damage in an early drought is relatively low and increases in later droughts with higher rates.

After adjustment of the drought damage considering the different factors discussed above, the cumulative probability of damage and the resulting values of HDI are calculated and applied for the prediction of drought severity using neural networks. The ANN models are used to forecast the status of drought in the next month based on the HDI which is a combined index of SPI, SWSI, and PDSI. In the following sections two ANN models are discussed.

Prediction of Drought Severity Using ANN Models

In the prior sections formulation and classification of the HDI have been discussed. Here, the relation of the HDI value for the next month and three drought indices of SPI, SWSI, and PDSI for the current month are estimated using two ANN models and drought severity is evaluated according to the classification of the HDI.

Multilayer Perceptron Neural Networks

The multilayer perceptron models have several layers (typically three layers) with processing units called “neurons.” In a neural network, each neuron works independently, therefore the behavior of the network is the sum of various neuron outputs. This property results in less local error in the output. In other words, neurons adjust themselves cooperatively which increases the robustness of the system. A specified neuron can generate a specified output for different inputs using transfer function.

The first step in using MLP networks is the determination of their architecture. Hornik et al. (1989) presented the principle of global approximation which indicates that a forward neural network with a sigmoid transfer function in the hidden layer and linear output layer is able to approximate many complicated problems. According to Hornik et al. (1989), the number of hidden layers can be decreased very efficiently, to obtain a less complicated network. The other factor which has an important role in the efficiency of the MLP models is the number of hidden layer neurons that can be determined using a trial and error procedure.

For training the model first the drought indices are rescaled to be consistent with the transfer functions and time series of indices. They are entered into the MLP model and subcategories of the HDI are obtained. For this purpose, in addition to changing the transfer functions and the number of neurons in the hidden layer, learning steps of the networks has been changed in the training stages of the model.

Probabilistic Neural Networks

The PNN models offer a way to interpret the network’s structure in terms of probability density functions (Berthold and Diamond 1998) as its important characteristics. The standard training procedure for these networks requires a single pass over all the patterns of the training set (Specht 1990). This characteristic makes the PNN models faster to train compared to feedforward neural networks.

The architecture of a PNN is limited to four layers: the input layer, the pattern layer, the summation layer, and the output layer, as illustrated in Fig. 3. A three-dimensional input vector including drought indices of SPI, SWSI, and PDSI, $X=(x_1, \dots, x_n)^T \in R^n$, $n=3$, is applied to the n input neurons and is passed to the pattern layer. The neurons of the pattern layer are divided into K groups, one for each subcategory of HDI. The i th pattern neuron in the k th group computes its output using a Gaussian kernel in the form of

$$F_{k,t}(X) = \frac{1}{(2\pi\sigma^2)^{n/2}} \exp\left(-\frac{\|X - X_{k,t}\|^2}{2\sigma^2}\right) \quad (10)$$

where $X_{k,t} \in R^n$ =center of the kernel; and σ , also known as the spread (smoothing) parameter, determines the size of the receptive field of the kernel. The summation layer of the network computes the approximation of the conditional class probability functions through a combination of the previously observed densities

$$G_k(X) = \sum_{t=1}^{M_k} \omega_{k,t} F_{k,t}(X), \quad k \in \{1, \dots, K\} \quad (11)$$

where M_k =number of pattern neurons of class k ; and $\omega_{k,t}$ =positive coefficients satisfying $\sum_{t=1}^{M_k} \omega_{k,t} = 1$. The pattern vector of indices, X , is classified as belonging to the subcategory of HDI ($C(X)$) which corresponds to the summation unit with the maximum output

$$C(X) = \arg \max_{1 \leq k \leq K} (G_k) \quad (12)$$

Case Study

The Gavkhooni/Zayandeh-rud basin in central Iran has been considered as the case study of this paper. This basin has five subbasins with a total area of 41,347 km². The dominant climate in the study area is arid and semiarid. The precipitation varies through-

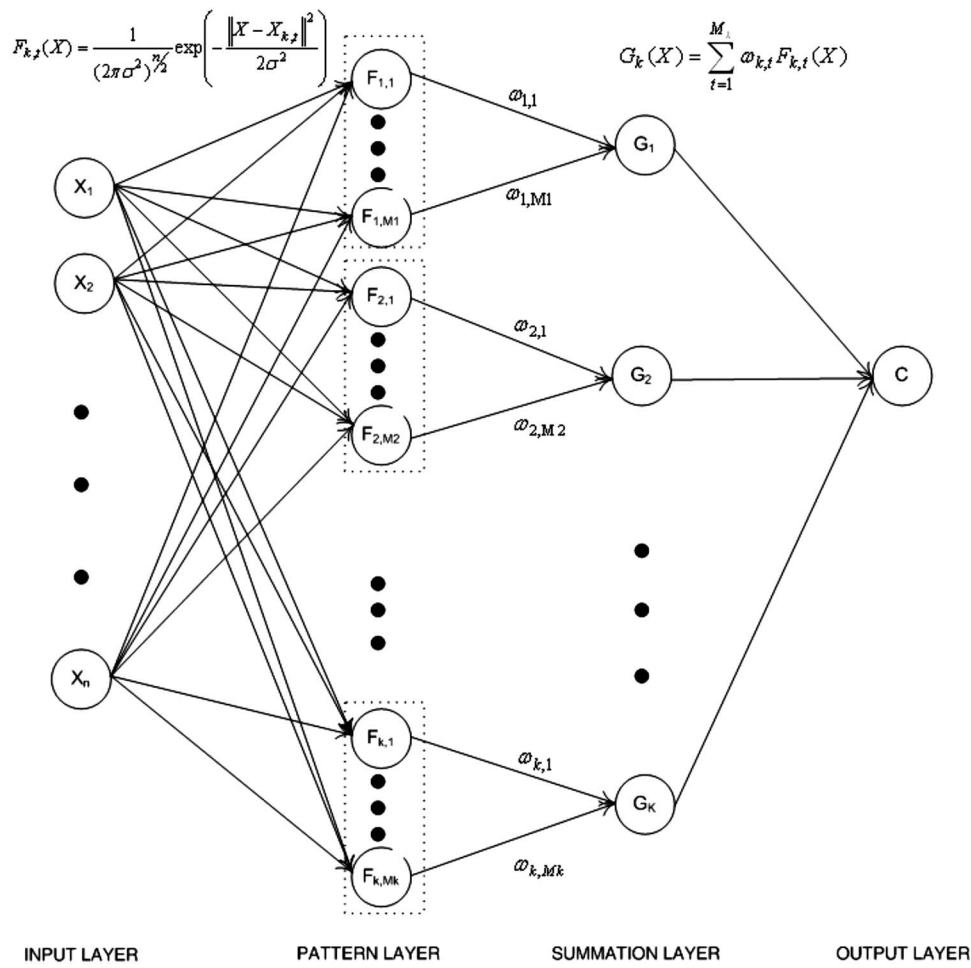


Fig. 3. Probabilistic neural network

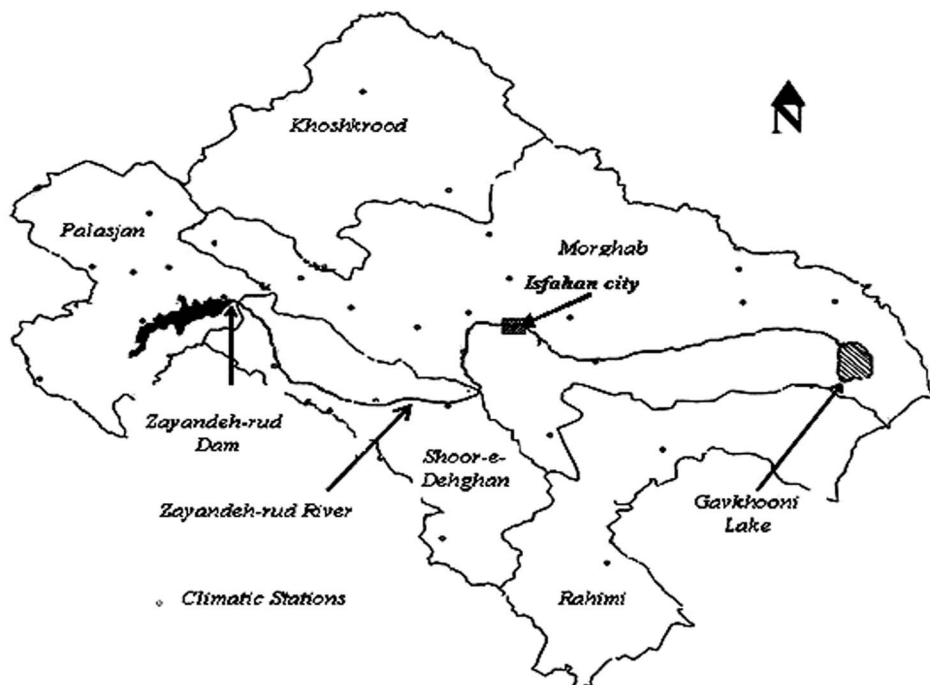


Fig. 4. Study area with subbasins and climatic stations

Table 2. Official Drought Damage Data in Study Area

Water year	Damage (million Rials)
1997–1998	94,475
1998–1999	176,558
1999–2000	1,035,287
2000–2001	1,573,260
2001–2002	2,055,162
2002–2003	871,183

out the basin between 2300 mm in the west (where most of the precipitation is in snow form) and 130 mm in the central part of Iran (where Isfahan city is located). Annual average precipitation in this basin is about 1,500 mm. The average precipitation in the Zayandeh-rud basin has been used for calculation of drought indices. The Zayandeh-rud River is the main surface resource for supplying the irrigation demands in this basin. As water and energy demands increase in Isfahan, water withdrawals from the river increase and it is important to incorporate climate variability into water resources decision making.

Table 3. Crop Sensitivity, $K_y^{i,j}$ and Area in Study Area

Crop	Wheat	Barely	Rice	Cotton	Sugar beet	Alfalfa	Green	Oil seeds	Beans	Onion and vegetable	Potato	Nuts	Other fruits	Other
January	0.5	0.5	0.5	—	—	—	—	—	—	—	—	—	—	1
February	0.5	0.5	0.5	—	—	—	—	—	—	—	—	—	—	1
March	1.1	1.1	1.1	—	—	—	—	—	—	—	—	—	—	1
April	0.4	0.4	0.4	—	—	—	—	—	—	—	—	—	—	1
May	0.4	0.4	0.4	0.15	0.15	0.15	0.5	—	—	—	—	—	—	1
June	—	—	—	0.15	0.15	1.15	1.5	—	0.5	0.6	0.5	0.8	0.8	1
July	—	—	—	1.1	1.1	1.15	0.5	0.5	0.85	0.75	0.85	1.1	1.1	1
August	—	—	—	1.1	1.1	0.15	—	1.2	1	—	1	1.1	1.1	1
September	—	—	—	0.15	0.15	0.15	—	0.5	0.5	—	0.5	0.8	0.8	1
October	—	—	—	0.15	0.15	—	—	—	—	—	—	0.5	0.5	1
November	0.4	0.4	0.4	—	—	—	—	—	—	—	—	—	—	1
December	0.4	0.4	0.4	—	—	—	—	—	—	—	—	—	—	1
Area for each crop (ha)	62,743	19,572	5,221	1,845	8,096	12,331	13,260	4,175	1,880	16,367	2,504	5,882	1,697	174,805

Table 4. Percentage of Agricultural Damage (AD) and Water Demands (WD)

Month	$\sum K_y \cdot A$	Total coverage area (ha)	K_y (weighted)	AD (%)	WD (%)
January	218,573	262,341	0.83	7.9	3
February	218,573	262,341	0.83	7.9	3
March	271,094.6	262,341	1.03	9.8	5
April	209,819.4	262,341	0.80	7.6	10
May	219,790.2	297,873	0.74	7.0	14
June	228,442.2	238,667	0.96	9.1	15
July	232,976.8	242,842	0.96	9.1	12
August	200,936.7	213,215	0.94	9.0	12
September	188,488.5	213,215	0.88	8.4	9
October	180,085.7	192,325	0.94	8.9	4
November	209,819.4	262,341	0.80	7.6	7
December	209,819.4	262,341	0.80	7.6	6

The Zayandeh-rud reservoir controls the streamflow with a volume of 1,470 million m^3 . The location of the Zayandeh-rud reservoir is shown in Fig. 4. The average annual inflow to Zayandeh-rud reservoir is about 1,600 $10^6 m^3$, of which an average flow of 600 million m^3 is transferred from the adjacent Karoon River basin. Drought trends in the basin have been studied between years 1971 and 2004 in this paper.

The Gavkhooni/Zayandeh-rud basin has special effects on the development and the economy of the region through agricultural, industrial, and tourism activities. Statistics show that the amount of precipitation, especially in the high altitudes from October 1999 to April 2000, has decreased approximately 35–45% compared to the long term average and resulted in 250 million m^3 water shortages in the Isfahan region in the year 2000.

Results

As the first step in the HDI calculations, monthly time series of SPI, modified SWSI, and PDSI are calculated from 1971 to 2004. In comparison to the meteorological and hydrological data, the

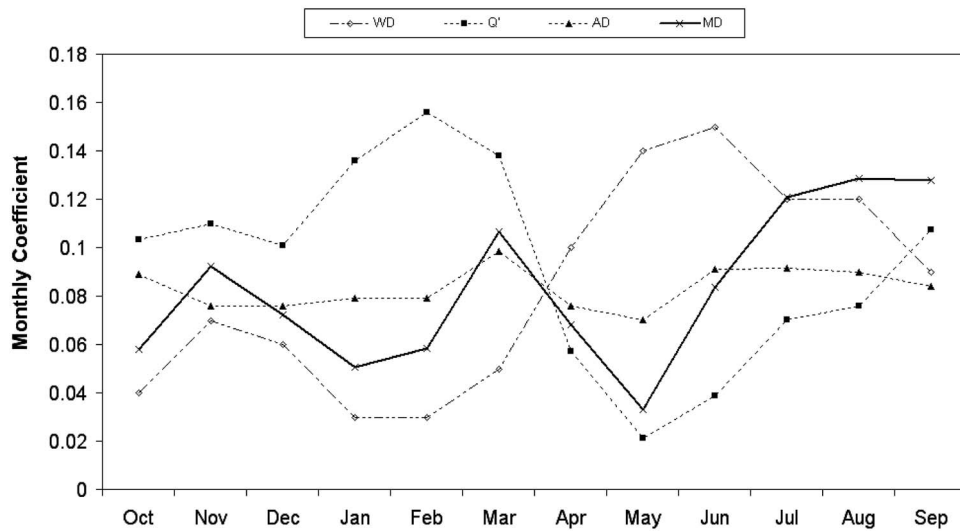


Fig. 5. Monthly changes on variables used for drought damage assessment

length of drought damage data is short and the data were available from October 1997 to September 2003 in an annual scale. Table 2 gives the data for drought damages in the study area reported officially by provincial governments of Isfahan and Kohkiluyeh va Boyer Ahmad. Eq. (4)–(9) are used for disaggregating the annual damage into monthly periods. The agricultural related variables include the crop type and sensitivity to soil water shortages, $K_y^{i,j}$ and coverage areas of crops in the study area are shown in Table 3. Using these variables, monthly agricultural damage, AD, is calculated. AD shows the overall sensitivity of the crops to the water shortage during a dry year considering the crop pattern. Table 4 gives the computation stages of AD. The maximum value of AD is in March because $K_y^{i,j}$ and crop area coverage in this month is high and it is the lowest in May. Even though crop area is higher in May than in March but it still has small AD due to the low $K_y^{i,j}$ in this month.

To evaluate the sensitivity of the study area during the shortages of water availability, the pattern of water demands, WD, and

reservoir outflow are considered. Monthly demands are shown in the last column of Table 4. Maximum water demand belongs to June when AD is also high and enough reservoir releases are needed in order to prevent the expectable damages. Q_i' shows the role of reservoir in supplying the demands which is calculated using Eq. (7). Fig. 5 illustrates monthly variation of Q_i' for the years 1999–2000 and its comparison to the other coefficients as is discussed before and MD. For better comparison, the values of Q_i' are rescaled by multiplying by a constant number. This figure shows that when water demand in a given month (e.g., February) is low, reservoir outflow is also low and consequently Q_i' is high and vice versa. Higher values of Q_i' address the higher damages. As shown in Fig. 5, the study area is very vulnerable to droughts in August and September. This is because the reservoir outflow in these months is low and crop variety and sensitivity to the water shortages is relatively high. In May, the least damage is expected because of the minimum agricultural damage, AD. It can be con-

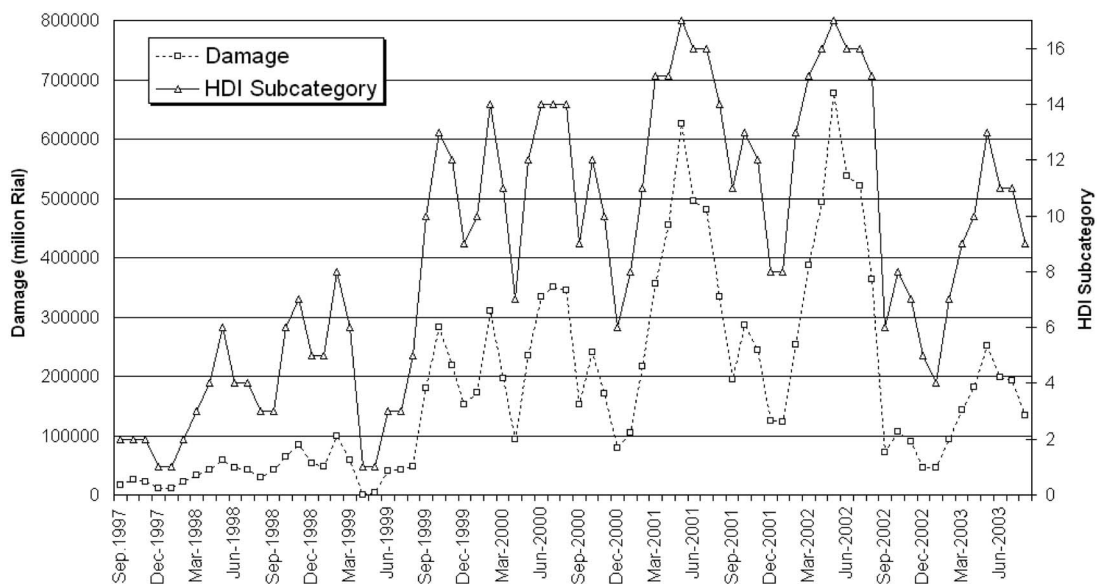


Fig. 6. Monthly time series of damage (converted to present values in year 2006)

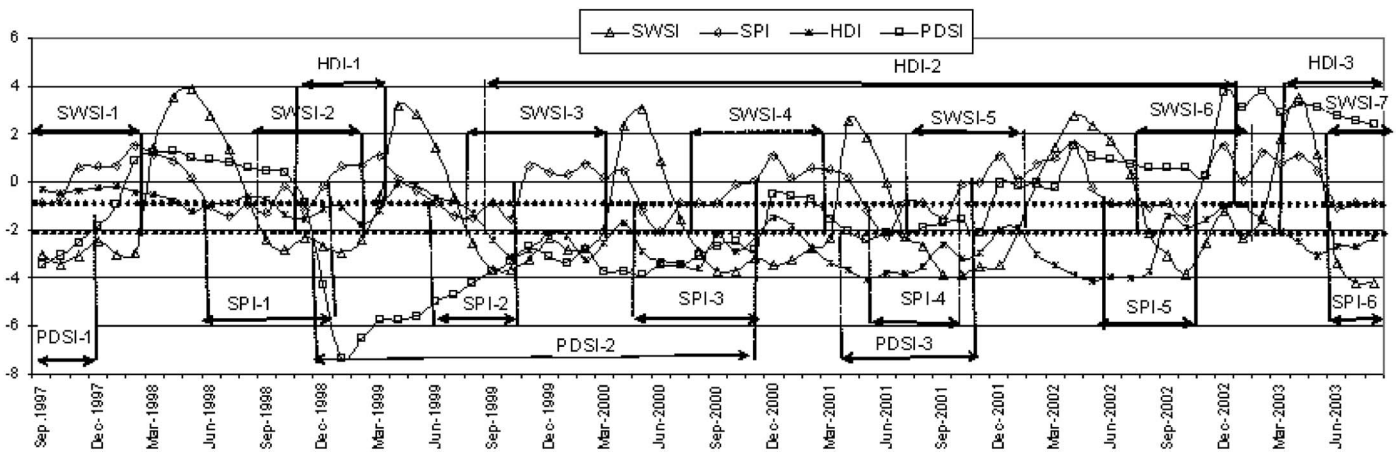


Fig. 7. Time series of three indices of drought in comparison to HDI

cluded that variables selected for drought analysis in this paper support each other very well and provide a combined view of drought.

Using the MD time series, annual damages are converted to the monthly steps but cannot yet be used to calculate HDI. First, the social setting factor, $\alpha_m(n_m)$ is applied in order to adjust the damage scores. In this study it is assumed that $\alpha_1(72)$ is 1.1. It means that in the region at the end of the 72nd dry month, 10% of potential drought damage has been prevented which should be added to the reported amounts in order to treat the severity of drought uniformly during the dry periods. Finally, the time series of damage is converted to year 2006 values for comparison purposes. The interest rate is considered as 17% based on the economical situation of the study area. The time series of monthly damages are shown in Fig. 6. According to the figure, the values of drought damage are gradually increased to get its higher amount and then declined to lower damages which reflects the nature of drought occurrence.

As mentioned in the calculation steps of HDI, the cumulative probability function of damage occurrences is developed using the Weibull probability distribution (Fig. 1) and used for determining the HDI values [Eq. (2)]. Different thresholds of drought severity according to the HDI, which are obtained from the probability-damage diagram, are also shown in Fig. 1.

The values of three indices (which indicate different climatic, hydrological, and agricultural aspects of drought) including SPI, SWSI, and PDSI as well as the hybrid index, HDI, have been calculated for the study area. The time series of these indices, their associated number of drought spans, and duration of dry periods are illustrated in Fig. 7. This figure shows that during the drought spans determined by HDI, in most of the cases three types of agricultural, climatic, and hydrological droughts have occurred. Furthermore, agricultural drought periods because of their gradual progress have lower frequencies but greater durations than those of hydrological and particularly meteorological droughts. In Table 5, the drought spans are compared and their overlapping periods with the HDI are shown. As can be seen, HDI can cover different aspects of drought including meteorological, hydrological, and agricultural. It also can be concluded that the hydrological and agricultural sectors have the main role in the magnitude of drought damages due to much more compatibility of drought periods according to the SWSI and PDSI as hydrological and agricultural drought indices with those reported by the HDI.

After determining time series of SPI, SWSI, PDSI, and HDI, the ANN models are developed for the prediction of drought severity in the next time step. Inputs of neural networks are the rescaled amounts of SPI, SWSI, and PDSI during the present month and their outputs are the number of HDI subcategories which show the drought severity for the next month. There are 17 subcategories due to the classification of HDI. Seventy percent of the monthly time series is used for training and the rest is used for validation of MLP and PNN models.

The MLP models with one hidden layer and *tansig* and linear transfer functions in hidden and output layers, respectively, that differ in neurons of hidden layer, are the better selected architecture. This architecture is used due to its widely accepted characteristics and for the purpose of developing the methodology. In order to compare the performance of models, the RMSE error index is used and the model with minimum RMSE in both calibration and validation periods is selected as the best model. RMSE is calculated as follows:

$$\text{RMSE} = \sqrt{\frac{\sum_{i=1}^n (\text{Obs}_i - \text{For}_i)^2}{n}} \times 100 \quad (13)$$

where Obs_i and For_i = observed and estimated data in month i , respectively. Using the above equation, the optimum architecture of MLP has been determined with six neurons in the hidden layer. According to the prediction results of the optimum MLP, this model has predicted the drought intensity correctly in 87.5% of the calibration and 54% of validation periods. The prediction error is 1.6 and 6.5 for calibration and validation periods,

Table 5. Durations of Drought Spans (Months)

Drought span's number	SPI	SWSI	PDSI	HDI
1	7	6	4	5
2		6	24	
3	5	8		40
4	7	8		
5	6	7	8	
6	5	6		
7	3	3		6
Overlapping with HDI	22	34	27	51

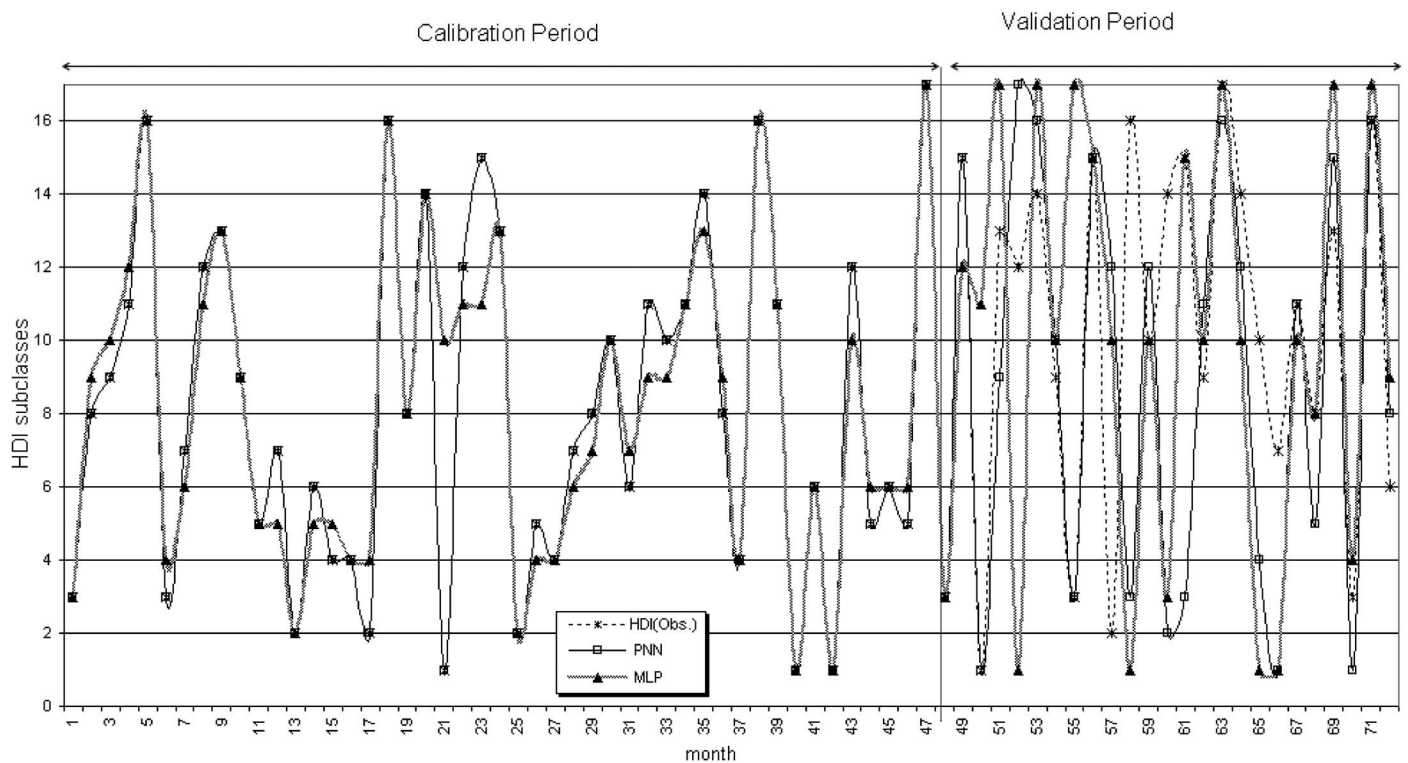


Fig. 8. Time series of calculated and the ANN predicted HDI

respectively. The time series of HDI forecasted by MLP are shown in Fig. 8.

The PNN models are very sensitive to the amount of data that is used for network construction. So for the developing of PNN model, the smoothing parameter of Gaussian kernel, σ , is modified and the better model has been selected based on the RMSE index. Fig. 9 shows that the lowest error happens when the value of σ ranges between 0.02 and 0.13. This network predicts severity of drought correctly in 59% of validation period and also in 77% with one class interval relaxation in the drought severity category with the prediction error of 5.7. The time series of HDI forecasted by PNN are compared with the results of MLP and time series of HDI are calculated directly from the recorded field data of dam-

age in Fig. 8. The results obtained through the PNN in the calibration period are the same as the values given for model training because of the special simulation method used in this kind of ANN models.

Generally in most cases, predictions using PNN are relatively better than those by using MLP. It has been proven that when there is adequate data available, the PNN models show better results. Better and more reliable damage data could improve the PNN results. Still the development and implementation of the methodology helps to encourage the agencies to develop better and more uniform strategies for collecting damage data. Perhaps implementation of drought insurance plans could help to gather adequate data which are a relative issue. It is difficult to say how

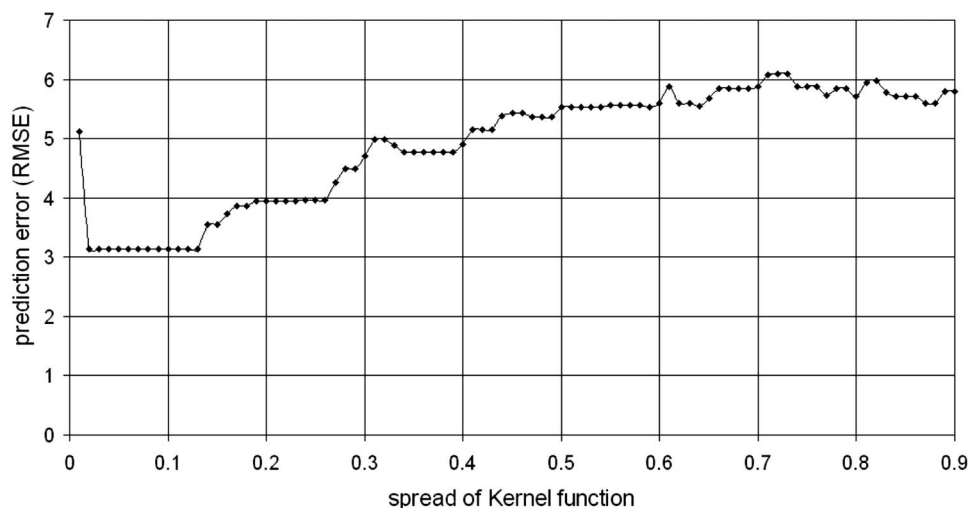


Fig. 9. Variations of RMSE with smoothing parameter of Kernel function

adequate “adequate” data are. An index similar to the Hurst coefficient which is a measure of long term persistence of data could help to determine the adequacy of data. The PNN models need more data for effective forecasting of HDI. On the other hand, better performance can be obtained from PNN in cases with longer drought damage data. However, the length of droughts during a 30-year period may be less than 10 years. Therefore the shortness of data is an inevitable issue. Using a run test to generate more data (say 500 years) could be an alternative. But it is widely accepted that the strength of the generated data is as much as the observed data.

Summary and Conclusion

In this paper, drought events have been evaluated using three indices for different types of droughts and a hybrid index is developed. The indices which have been used for this purpose are: (1) SPI, as the index of meteorological drought; (2) SWSI, as the index of hydrological drought; and (3) PDSI as the index of agricultural drought. Due to limitations of these indices in drought assessment, and for the purpose of mitigating their shortcoming, the HDI has been developed using SPI, SWSI, and PDSI and also the recorded drought damage. Drought periods that are determined using the HDI have been compared with drought periods assessed based on the three other indices of drought. The proposed hybrid index in comparison with the other indices has shown to a better performance for the case study. This index implicitly considers the combination of climatic and economic variables, by assessing drought damages. According to the results of this study, agricultural drought has the highest share of drought damages. Having three time series of drought indices and HDI, the MLP and PNN models have been used to predict the HDI based on three drought indices. These ANN models take the three drought indices in the present month as inputs and predict HDI for the next month as output. In comparison with MLP models, the PNN model shows relatively better results and has predicted the drought severity correctly in 59% of the validation period. The ANN models need more data for effective forecasting of HDI and the lack of adequate classified damage data in this study is one of the reasons for average performance of MLP.

It can be concluded that using drought damage based HDI could help the governors to study and predict the probable drought severity and damage comprehensively according to the special meteorological, hydrological, agricultural, social, and economical characteristics of the study region. The methodology presented in this paper could be very useful in mitigating droughts with the higher values of damage.

Acknowledgments

This paper was partially funded by the Office of Research at the University of Tehran.

References

- Alley, W. M. (1984). “The Palmer drought severity index: Limitations and assumptions.” *J. Clim. Appl. Meteorol.*, 23, 1100–1109.
- Berthold, M., and Diamond, J. (1998). “Constructive training of probabilistic neural networks.” *Neurocomputing*, 19, 167–183.
- Chang, G. (1990). “Effects of droughts on the streamflow characteristics.” *J. Irrig. Drain. Eng.*, 116(3), 332–341.
- Chen, S., Cowan, C. F. N., and Grant, P. M. (1991). “Orthogonal least squares learning algorithm for radial basis function networks.” *IEEE Trans. Neural Netw.*, 2(2), 302–309.
- Clausen, B., and Pearson, C. P. (1995). “Regional frequency analysis of annual maximum streamflow drought.” *J. Hydrol.*, 173, 111–130.
- Cohen, S., and Intrator, N. (2002). “A hybrid projection-based and radial basis function architecture: Initial values and global optimisation.” *Pattern Anal. Appl.*, 5(2), 113–120.
- Dracup, J. A., Lee, K. S., and Paulson, E. G. (1980). “On the definition of droughts.” *Water Resour. Res.*, 16(2), 297–302.
- Eltahir, E. A. B. (1992). “Drought frequency analysis of annual rainfall series in central and western Sudan.” *J. Hydrol. Sci.*, 37(3), 185–199.
- Frick, D. M., Bode, D., and Salas, J. D. (1990). “Effects of drought on urban water supplies. I: Drought analysis.” *J. Hydraul. Eng.*, 116(6), 733–753.
- Garen, D. (1993). “Revised surface water supply index for western United States.” *J. Water Resour. Plann. Manage.*, 119(4), 437–454.
- Hornik, K., Stinchcombe, M., and White, H. (1989). “Multilayer feed-forward network are universal approximators.” *Neural Networks*, 2, 359–366.
- Karamouz, M., Rasavi, S., and Araghinejad, Sh. (2004a). “Application of artificial neural networks in flood estimation.” *Proc., 4th Int. Conf. on Decision Making in Urban & Civil Engineering*, Porto, Portugal.
- Karamouz, M., Torabi, S., and Araghinejad, Sh. (2004b). “Analysis of hydrologic and agricultural droughts in central part of Iran.” *J. Hydrol. Eng.*, 9(5), 402–414.
- Karamouz, M., Torabi, S., and Araghinejad, Sh. (2007). “Case study of monthly regional rainfall evaluation by spatiotemporal geostatistical method.” *J. Hydrol. Eng.*, 12(1), 97–108.
- McKee, T. B., Doesken, N. J., and Kleist, J. (1993). “The relationship of drought frequency and duration to time scales.” *Preprints, Proc., 8th Conf. on Applied Climatology*, American Meteorological Society, Anaheim, Calif., 179–184.
- Miravet, C., and Rodriguez, F. B. (2003). “A hybrid MLP-PNN architecture for fast image superresolution.” *Lect. Notes Comput. Sci.*, 2714, 178–179.
- Palmer, W. C. (1965). “Meteorological drought.” U.S. Weather Bureau, *Research Paper No. 45*, Washington, D.C.
- Pinkayan, S. (1966). “Conditional probabilities of occurrence of wet and dry years over a large continental area.” *Hydrology Paper 12*, Colorado State Univ., Fort Collins, Colo.
- Rouhani, S., and Cargile, A. K. (1989). “A geostatistical tool for drought management.” *J. Hydrol.*, 108, 257–266.
- Santos, M. A. B., Correia, F. N., and DaCunha, L. V. (1983). “Drought characterization and drought impacts in Portugal.” *Memoria 591*, Laboratorio Nacional de Engenharia Civil, Lisbon, Portugal.
- Sen, Z. (1980). “Regional drought and flood frequency analysis: Theoretical consideration.” *J. Hydrol.*, 46, 265–279.
- Shafer, B. A., and Dezman, L. E. (1982). “Development of a surface water supply index (SWSI) to assess the severity of drought conditions in snow pack runoff area.” *Proc., Western Snow Conf.*, Colorado State University, Fort Collins, Colo., 164–175.
- Shin, H. S., and Salas, J. D. (2000). “Regional drought analysis based on neural networks.” *J. Hydrol. Eng.*, 5(2), 145–155.
- Specht, D. F. (1990). “Probabilistic neural networks.” *Neural Networks*, 1(3), 109–118.
- Specht, D. F., and Romsdahl, H. (1994). “Experience with adaptive probabilistic neural network and adaptive general regression neural network.” *Proc., IEEE World Congress on Computational Intelligence*, Orlando, Fla., 2, 1203–1208.
- Tase, N. (1976). “Area-deficit-intensity characteristics of drought.” Ph.D. dissertation, Colorado State Univ., Fort Collins, Colo.
- Wang, D. C., and Salas, J. D. (1989). “Stochastic modeling and generation of droughts,” *Proc., ASCE National Conf. on Hydraulic Engineering*, New Orleans, August 14–18, 1989, ASCE, New York, 50–57.
- Zelenhasic, E., and Salvai, A. (1987). “A method of streamflow drought analysis.” *Water Resour. Res.*, 23(1), 156–168.